

# The Study of Squeezing Unstable $Fe_3O_4$ and $TiO_2$ -Nanofluid Flow Due to The Radiant Heating and Thermal Generation /Absorption

A. G. Madaki<sup>\*, 1</sup>, M. M. Amina<sup>2</sup>, S. K. Alaramma<sup>3</sup>, C. S. K. Raju<sup>4</sup>, A. A Hussaini<sup>5</sup>

<sup>1,3,5</sup> Department of Mathematical Sciences, Abubakar Tafawa Balewa University, PMB 0248, Bauchi, Nigeria.

<sup>2</sup> Aminu Saleh College of Education, PMB 044 Azare, Bauchi State, Nigeria.

<sup>4</sup> Department of Mathematics, VIT University, Vellore-632014, India

**Abstract:-** In this study, a numerical investigation of squeezing transient nanofluids flow between two parallel plates are considered. The impacts of radiant heating and thermal generation/absorption across the temperature profile were scrutinized. The Runge-Kutta fourth-order method (RK4) with shooting scheme was used to solve the two-dimensional non-linear momentum and energy equations. It is perceived that, incrementing the radiative parameter results in a decrease in the temperature profile, while the fluid thermal reading is vividly ascending in the cause of thermal generation but diminishes in the cause of thermal absorption respectively. The result shows a fascinating and reasonable agreement between the nano-sized  $Fe_3O_4$  and  $TiO_2$ , though, a slight high upturn in thermal boundary layer thickness with  $TiO_2$  is spotted than that of  $Fe_3O_4$ .

**Key words:-** Non-linear equations, Parallel plates, ODEs, Runge-Kutta scheme (RK4)

## List of Abbreviations

IVP – Initial Value Problem

ODEs – Ordinary Differential Equations

HAM – Homotopy Analysis Method

## 1. INTRODUCTION

Substantial functioning thermal transport fluid models are the topic of numerous scrutinization in current decades. due to the esteem thermal conductivities' properties of metals, the thermal conductivity of suspensions of gritty solid in liquids have been an exciting research field for its enormous extent of physical instruments in many industrial and engineering processes. Many publications illustrate the present and prospective utilization of nanofluids Saleh, et al. (2017). Nanofluid has diverse applications in engineering and geophysical sciences. Among these comprises cooling of nuclear reactors, cooling of electronic equipment, and solar energy collectors, etc.

The flow of fluid and thermal transport via an unbounded upright plate has vast applications in science and technology. Amongst which involve packed-bed storehouse tanks and catalytic reactors etc. Lai et al. (1991) have analyzed the problem of nanofluid flow across an upward plate in the proximity of time exponential temperature on the boundary, their result shows that the nano particle concentration improves for fluids with little thermal conductivity while the fluid temperature is reducing. Some rich number of studies in relation to the nanofluid flow with different solid particles via indistinct geometries were found in Chamkha, (2002), Umarathai et al. (2005), Salma et al. (2012), Ghalambaz et al. (2019), Raza et al. (2019), Kumar et al. (2019), Chamkha et al. (2019), Toghraie et al. (2020), Molana et al. (2020), Dogonchi et al. (2020), and Nirmalendu et al. (2021). Sheikholeslami et al. (2013) intensively carried out their research in relation to the squeezed unstable fluid flow using fourth-order Runge-Kutta (RK4). Nonetheless, some other fascinating and associated study is detailed in Hamza (1991). A scintillating research on the radiant heating was conducted in Kandasamy et al. (2013). Radiations perform an important task in heat transfer, as such, many researchers have carried out pieces of research on it. Hayat et al. (2013) have presented radiant heating impact in squeezing flows of Jeffery fluids. Alsaedi et al. (2012) studied the thermal generation/absorption impact within the standstill fluid flow.

Hussaini et al. (2018) examined Bioconvection model for squeezing flow within likeness plates bearing gyrotactic microorganisms with the influence of radiant heat and thermal generation/absorption by using HAM.

Moreover, the impacts of thermal generation/absorption were sufficiently examined and reported by Srinivasa and Eswara (2016), Abdel-wahed et al. (2015) and Madaki et al. (2018), respectively.

The goal of this study is to use Runge-Kutta fourth order method (RK4) along with shooting technique to procure the numerical solution of squeezing unsteady  $Fe_3O_4$  and  $TiO_2$ -nanofluid flow in the presence of radiant heating and thermal generation /absorption.

The radiant heat as well as thermal generation/absorption effect were analyzed on the thermal profile. Conversely, the numerical result obtained for missing parameters  $f'(0)$ ,  $f'''(0)$ ,  $\theta(0)$  for  $Fe_3O_4$  were compared with previous result obtain by Madaki et al. (2018) using fourth-order Runge-Kutta with shooting technique for Cu-water.

## 2. DESCRIPTION OF THE PROBLEM

The behavior of unstable nanofluid squeezed within two evenly spaced plates were perceived in this research. The space within the two plates at any dimensionless time  $t$  is stated as  $\omega = \pm l(1 - \alpha t)^{\frac{1}{2}} = \pm h(t)$  where  $w$  is the distance,  $\alpha$  is constant, and  $l$  is original ground (at  $t = 0$ ). The flow model is deliberated along  $x$  and  $y$  axis and  $z$  is the axial correspondent which is studied to be zero from the flow province, the viscous distribution influence and thermal source due to friction were fastened.

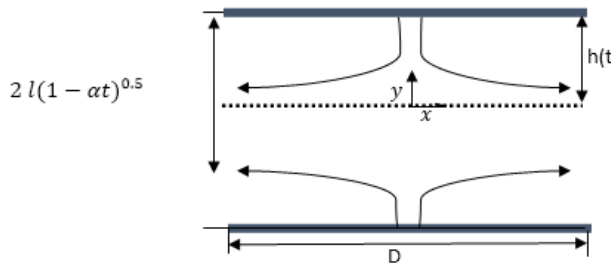


Figure 1: Physical model of the problem

The Runge-Kutta fourth order (RK4) with shooting scheme will be utilized on the modified nonlinear ODEs to examine the impression of both radiant heating and the thermal generation/absorption along with other parameter on the estimated solution of unsteady squeezing of  $Fe_3O_4$  and  $TiO_2$ - nanofluid flow within the two parallel plates. Hence the fluid is nanofluid which comprised both ferrofluid and  $TiO_2$ .

$$\frac{\partial u}{\partial x} + \frac{\partial v}{\partial y} = 0 \quad (1)$$

$$\frac{\partial u}{\partial t} + u \frac{\partial u}{\partial x} + v \frac{\partial u}{\partial y} = -\frac{1}{p_{nf}} \frac{\partial p}{\partial x} + \frac{\mu_{nf}}{p_{nf}} \left( \frac{\partial^2 u}{\partial x^2} + \frac{\partial^2 u}{\partial y^2} \right) \quad (2)$$

$$\frac{\partial v}{\partial t} + u \frac{\partial v}{\partial x} + v \frac{\partial v}{\partial y} = -\frac{1}{p_{nf}} \frac{\partial p}{\partial y} + \frac{\mu_{nf}}{p_{nf}} \left( \frac{\partial^2 v}{\partial x^2} + \frac{\partial^2 v}{\partial y^2} \right) \quad (3)$$

$$\frac{\partial T}{\partial y} + v \frac{\partial T}{\partial x} + u \frac{\partial T}{\partial y} = \frac{k_{nf}}{(\rho C_p)_{nf}} \left( \frac{\partial^2 T}{\partial x^2} + \frac{\partial^2 T}{\partial y^2} \right) + \frac{\mu_{nf}}{(\rho C_p)_{nf}} \left[ 4 \left( \frac{\partial u}{\partial x} \right)^2 + \left( \frac{\partial v}{\partial x} + \frac{\partial u}{\partial y} \right)^2 \right] - \frac{1}{\rho C_p} \frac{\partial q_r}{\partial y} + \frac{Q(T - T_\infty)}{\rho_{nf}} \quad (4)$$

The boundary conditions are assumed in the form:

$$v = v_w = \frac{dh}{dt}, \quad T = T_H \text{ at } y = h(t),$$

$$v = \frac{\partial u}{\partial y} = \frac{\partial T}{\partial y} = 0 \text{ at } y = 0. \quad (5)$$

where  $u$  and  $v$  serve as the velocities in  $x$  and  $y$  guidance, sequentially. whilst  $p$ ,  $T$ ,  $T_\infty$ ,  $f$ ,  $\rho$  and  $Q$  are the pressure, the fluid temperature, an outline temperature, the fluid, the density and the thermal generation/absorption coefficient, respectively, and  $\rho_{nf}$ ,  $\mu_{nf}$ ,  $(\rho C_p)_{nf}$  and  $K_{nf}$  are appropriately the effective density, dynamic viscosity, heat capacity, and thermal conductivity of the nanofluid as expressed by Domairry and Aziz (2009).

The Effective dynamic viscosity of nanofluid is given by

$$\mu_{nf} = \frac{\mu_f}{(1 - \varphi)^{2.5}}$$

where  $\varphi$  is the solid volume fraction of nanoparticles. The effective density,  $\rho_{nf}$ , thermal diffusivity  $\alpha_{nf}$ , and the heat capacitance of the nanofluid is provided as

$$\rho_{nf} = (1 - \varphi)\rho_f + \varphi\rho_s$$

$$\alpha_{nf} = \frac{K_{nf}}{(\rho C_p)_{nf}}$$

$$(\rho C_p)_{nf} = (1 - \varphi)(\rho C_p)_f + \varphi(\rho C_p)_s$$

The thermal conductivity of nanofluids restricted to spherical nanoparticles is approximated by Max-well Garnett model

$$K_{nf} = \frac{k_f[k_s + 2k_f - 2\varphi(k_f - k_s)]}{[k_s + 2k_f - \varphi(k_f - k_s)]} \quad (6)$$

The subscripts  $nf$ ,  $f$ , and  $s$  described thermophysical characteristics of the nanofluid, base fluid, and nano-solid materials respectively.

**Table 1.0**

Thermophysical properties of the fluid and solid particles

Physical Properties	Fluid phase (water)	Titanium Oxide (TiO <sub>2</sub> )	Iron (II, III) Oxide (Fe <sub>3</sub> O <sub>4</sub> )
$C_p$ (j/Kg k)	4179	686.2	670
$\rho$ (Kg/m <sup>3</sup> )	997.1	4250	5810
$K$ (W/mK)	0.613	8.9538	80.4

$q_r$  is the radiation heat fluctuation, is express by Stefan-Boltzmann law as the radiation energy per unit time from a body is proportional to the fourth power of the absolute temperature i.e.

$q_r = \sigma T^4 A$  where  $q$  is the heat transfer per unit time ( $\omega$ ),  $\sigma$  is the Stefan Boltzmann constant,  $T$  is the absolute temperature,  $A$  is the Area of the emitting body.

However, the radiative heat flux term appeared in equation (4) has also vividly communicated by Roseland (1931) as  $q_r = -\frac{4\sigma^* \partial T^4}{3k^* \partial y}$  (7)

Regarding some studies by Akbar et al. (2013), and Kothandapani and Prakash (2015) consider that the temperature disparity amid the flow is substantially confined, and the term  $T^4$  can be weighed as a linear function of temperature. Hence,  $T^4$  is broadened employing Taylor series expansion around  $T_\infty$  and neglecting the higher-order constants, we have

$$T^4 = T_\infty^4 + 4T_\infty^3 T - 4T_\infty^4 \quad (8)$$

$$T^4 = 4T_\infty^3 T - 3T_\infty^4$$

Substituting eqs. (7) and (8) into (4)

$$\frac{\partial T}{\partial y} + v \frac{\partial T}{\partial x} + u \frac{\partial T}{\partial y} = \frac{k_{nf}}{(\rho c_p)_{nf}} \frac{\partial^2 T}{\partial x^2} + \frac{\partial^2 T}{\partial y^2} + \frac{k_{nf}}{(\rho c_p)_{nf}} \left[ 4 \left( \frac{\partial u}{\partial x} \right)^2 + \left( \frac{\partial v}{\partial x} + \frac{\partial u}{\partial y} \right)^2 \right] - \frac{1}{\rho c_p} \frac{32\sigma^*}{3k^*} \frac{\partial T_\infty^3}{\partial y} \frac{\partial^2 T}{\partial y^2} + \frac{Q(T - T_\infty)}{\rho_{nf}} \quad (9)$$

Introducing the following non-dimensional quantities as in Madaki et al (2018),

$$\omega = -\frac{\alpha x}{2l \left[ \left( (1-\alpha t)^{\frac{1}{2}} \right)^3 \right]} f''(\eta), \quad \eta = \frac{y}{l(1-\alpha t)^{\frac{1}{2}}}, \quad u = \frac{\alpha x}{[2(1-\alpha t)]} f'(\eta), \quad v = -\frac{\alpha l}{[2(1-\alpha t)]} f(\eta), \quad \theta(\eta) = \frac{T}{T_H}, \quad N = \frac{4\sigma^* T_\infty^3}{K_f \rho c_p K^*}, \quad \lambda = \frac{Q2l(T_w - T_\infty)(1-\alpha t)}{K_f \rho_f T_w}, \quad A_1 = (1 - \varphi) + \varphi \frac{\rho_s}{\rho_f}, \quad A_2 = (1 - \varphi) + \varphi \frac{(\rho c_p)_s}{(\rho c_p)_f}, \quad A_3 = \frac{k_{nf}}{K_f}, \quad (10)$$

And replacing the dimensionless quantities in equation (10) inside Eqs. (2) - (4) and getting rid of the pressure gradient from the summing eqs. (2) and (3) yields the following similarity equations (11) and (12).

$$f^{iv}(\eta) - SA_1(1 - \varphi)^{2.5} (3f''(\eta) + \eta f'''(\eta) + f'(\eta)f''(\eta) - f(\eta)f'''(\eta)) = 0 \quad (11)$$

$$(-12A_3K_f + 16A_2N)\theta'' - 3p_r SA_2(f\theta' + \eta\theta') + \frac{3p_r Ec}{(1-\varphi)^{2.5}} (f''^2 - 4\delta^2 f'^2) + 3\lambda A_2\theta = 0 \quad (12)$$

Using the following quantities as defined by Mustafa et al. (2012)  $S$  is the squeeze number,  $Pr$  and  $Ec$  are the Prandtl and Eckert integers, respectively

$$p_r = \frac{\mu_f(\rho c_p)_f}{\rho_f k_f}, \quad S = \frac{\alpha l^2}{2v_f}, \quad Ec = \frac{\rho_f}{(\rho c_p)_f} \left( \frac{\alpha x}{2(1-\alpha t)} \right)^2, \quad \delta = \frac{1}{x} \quad (13)$$

Equation (11) and (12) have to be solved subject to the following conditions

$$f(0) = 0, f''(0) = 0, f(1) = 1, f'(1) = 0, \theta'(0) = 0, \theta(1) = 1 \quad (14)$$

### 3. Method of solution with Runge-Kutta fourth order along with shooting technique

The similarity equations (11) and (12) along with boundary condition (14) were solved using shooting technique by converting it into an IVP. Therefore, we set

$$f' = u, u' = f'' = v, v' = f''' = w, w' = f^{iv}, \theta' = r(\eta), r'(\eta) = \theta''(\eta) \quad (15)$$

With the boundary conditions

$$f(L) = 1, u(L) = 0, \theta(L) = 1 \quad (16)$$

using Runge-Kutta fourth order scheme, a suitable guess values for  $f''(0), f'''(0), \theta(0)$  were made until the boundary condition at infinity  $f''(\infty), f'''(\infty), \theta(\infty)$  decay exponentially to zero. This computation is done with the aid of shootlib function in maple software. The effect of thermal radiation and heat generation/absorption in nanofluid flow squeeze through two parallel plate has been studied for different values of squeezing integer, radiation parameter, volume fraction of nano particles, temperature profile together with other salient parameters like the Prandtl number ( $Pr$ ), Eckert number ( $Ec$ )

### 5. RESULTS AND DISCUSSION

The maturation of the mathematical representation of the compressed unstable nanofluid flow via the equidistant plates as manifested in Fig. 1, where the significant impact of the radiant heating and the thermal generation/absorption variables beside an appropriate parameter on the flow and heat transfer peculiarities have been analyzed numerically. We have used the Runge-Kutta fourth order with shooting method to solve the corresponding governing equations. Consequently, the missing parameters  $f'(0), f'''(0), \theta(0)$  have been reckoned, where both the velocity and temperature profiles were analyzed and they were secured using RK4 scheme with shooting technique as presented in **table 3**.

Table 2a: Impact of  $\lambda$  on  $\theta(1)$  (for  $Fe_3O_4$ ) when  $s = 1, Ec = 0.5.5, Pr = 6.2, N = 0.5, \varphi = 0.02$ , and  $\delta = 0.01$ .

$\lambda$	0.0	0.5	1.0	3.0	5.0
$\theta(1)$	1.1071	1.1791	1.2591	1.6951	2.4796

Table 2b: Impact of  $\lambda$  on  $\theta(1)$  (for  $TiO_2$ ) when  $s = 1, Ec = 0.5.5, Pr = 6.2, N = 0.5, \varphi = 0.02$ , and  $\delta = 0.01$ .

$\lambda$	0.0	0.5	1.0	3.0	5.0
$\theta(1)$	1.1083	1.1805	1.5424	1.8275	8.5288

Table 3: Comparison for the numerical result obtain for missing parameters between the present study and existing result by Madaki et al. (2018).

Parameters	Madaki et al. (2018)	Present study
$f'(0)$	1.41582016	1.42065576
$f'''(0)$	-2.01604099	-2.06975916
$\theta(0)$	1.11883156	1.23192988

From Table 2a and 2b its observed that the increase in heat generation parameter initiate a slight increase in the temperature profile. Showing that for both  $TiO_2$  and  $Fe_3O_4$  the fluid temperature is proportionally and physically rising with heat generation parameter, and it is also observed that there is much rise of the fluid temperature with  $TiO_2$ -water than  $Fe_3O_4$ -water.

Table 3 depicts the comparison of result obtained by Madaki et al. [22] of Cu-water and the present study ( $Fe_3O_4$ -water). With  $S = 1, N = 0.5, Ec = 0.010, Pr = 6.20, \varphi = 0.020, \delta = 0.010, \lambda = 1.5$ , the result shows a convincing agreement between the value of the missing parameters  $f'(0), f'''(0)$  and  $\theta(0)$  of Cu-water and  $Fe_3O_4$ -water, respectively.

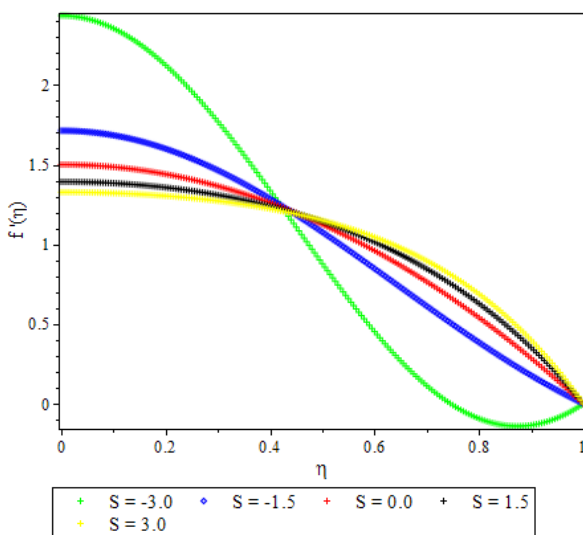


Figure 2: Influence of squeeze number on the velocity profile ( $TiO_2$ ).

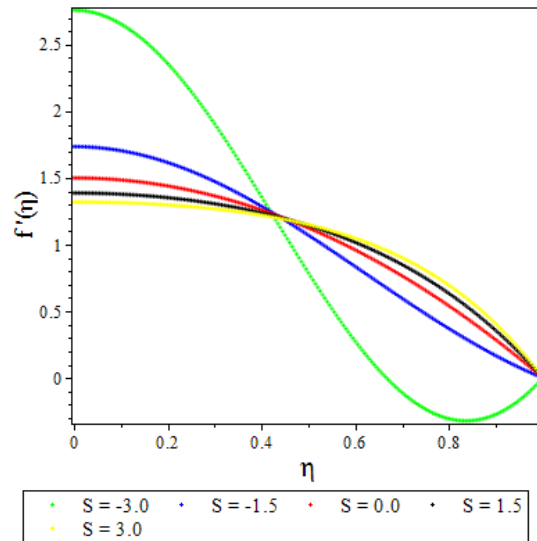


Figure 3: Influence of squeeze number on the velocity profile ( $Fe_3O_4$ ).

In figures 2 and 3, it is observed that both (+ and -) squeezed characters have dissimilar influences on the velocity profile. The squeeze number  $S$ , shows the movement of the plates, which implies when  $S > 0$  it matches with the plates traveling independently, whilst  $S < 0$  it relates with the plates progressing jointly. However, it shows that both  $Fe_3O_4$  and  $TiO_2$  have mutual agreement with the motion of the plates.

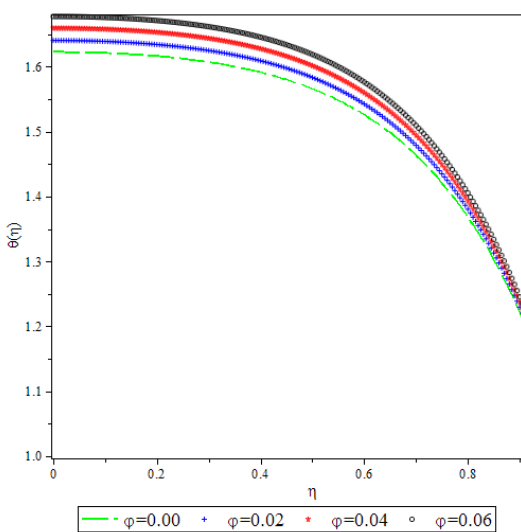


Figure 4: Impact of volume fraction of nanoparticle on the thermal profile ( $TiO_2$ ).

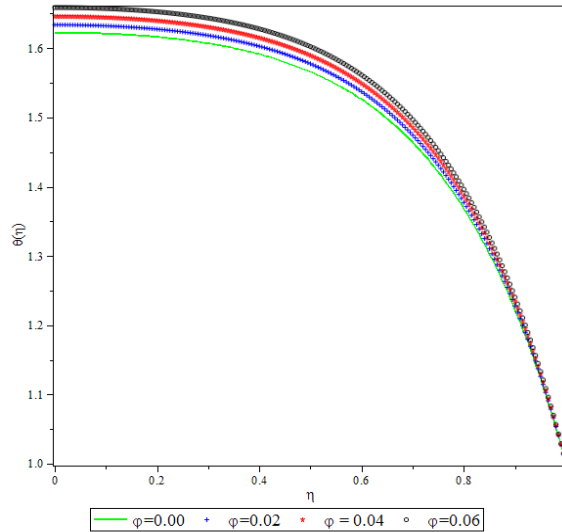


Figure 5: Impact of volume fraction of nanoparticle on the thermal profile ( $Fe_3O_4$ ).

Figures 4 and 5 show that for both  $Fe_3O_4$  and  $TiO_2$ , as the magnitude of nano particles is added into the traditional fluid, this gives rise in thermal boundary layer thickness. It is noticeable that on growing in the values of volume of solid particle the velocity boundary layer is leaned near the proximity of the plates, while remote from the surface of the plates it progressed, owing to the great thermal conductivity of the solid particle, the heat transfer is believed to have been improved, while the thermal profile is anticipated to have been declined. It is also noticed that the rise in thermal boundary layer thickness tends to occur faster with  $TiO_2$  than  $Fe_3O_4$  when the parameter is being increased.

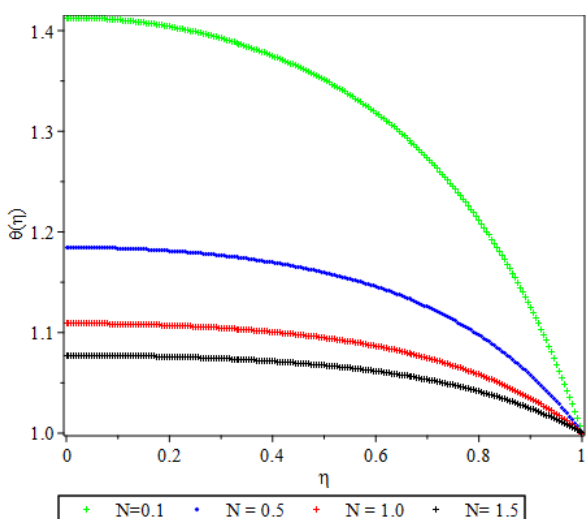


Figure 6: Impact of radiant heating on  $\theta(\eta)$  ( $TiO_2$ -water).

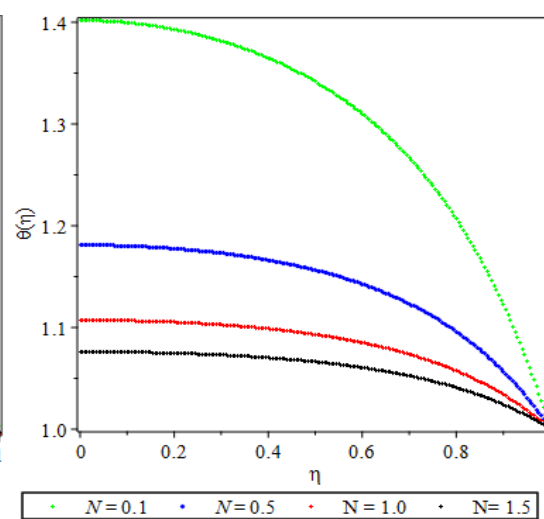


Figure 7: Impact of radiant heating on  $\theta(\eta)$  ( $Fe_3O_4$ - water).

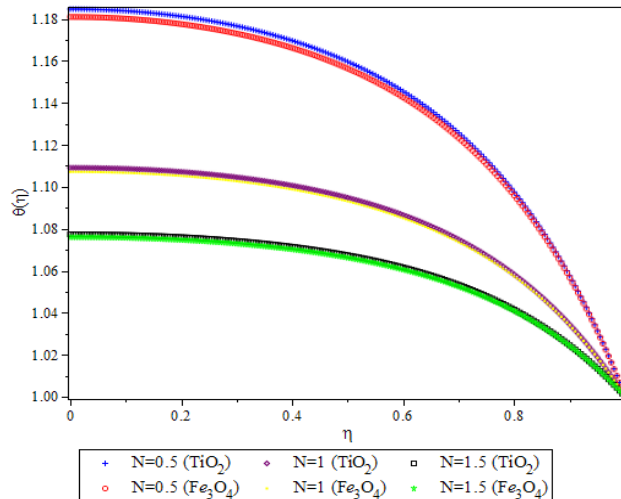
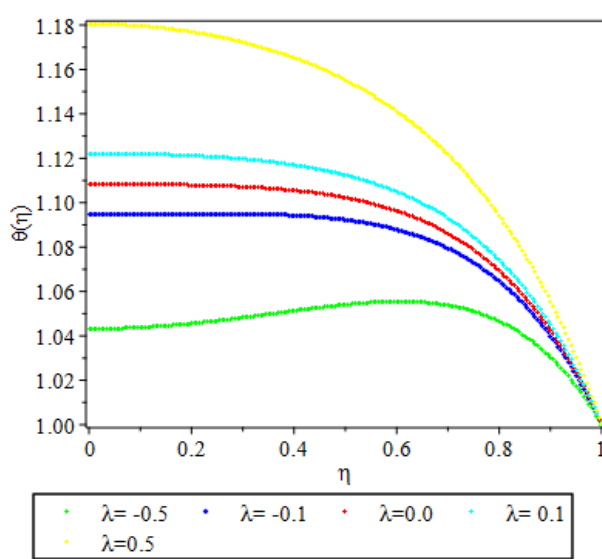


Figure 8: The radiant heating influence on the  $\theta(\eta)$  of the combined result with both  $Fe_3O_4$  and  $TiO_2$ .

From figures 6 and 7, the curves show that the fluid temperature is significantly reduced with a bit increment in the radiant heating integer  $N$  for every value of  $\theta(\eta)$  as well as the thermal boundary layer width that is heat transfer coefficient continuously decreases. Meaning that, the nanofluid temperature profiles are influenced by radiant heating integer  $N$  for the fixed values of governing parameters.

**Figure 8** shows the mutual agreement between  $Fe_3O_4$  and  $TiO_2$  where it's also vividly noticed that the temperature profile decreases slightly fast with  $Fe_3O_4$  than  $TiO_2$  when  $N$  is being increased.



**Figure 9:** Heat source influence on  $\theta(\eta)$   
 $(TiO_2$ -water).

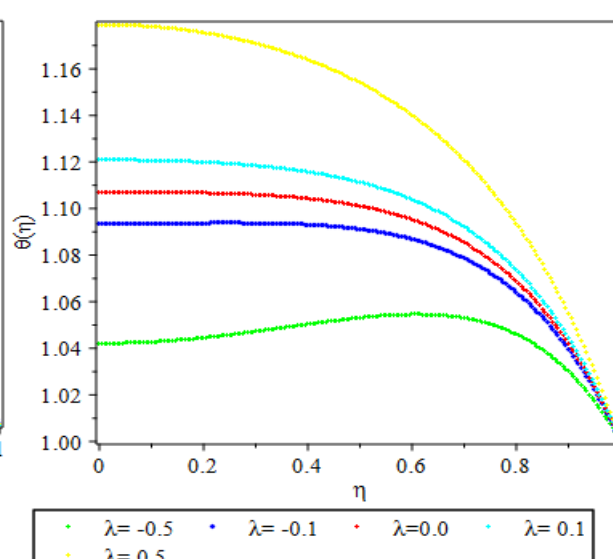


**Figure 10:** Heat source influence on  $\theta(\eta)$   
 $(Fe_3O_4$ - water).

In Figures 9 and 10, the curves exhibit the heat source influence on the thermal profile, it is observed that with  $(\lambda > 0)$  implying heat generation, there is increase in the fluid physical temperature. While with  $(\lambda < 0)$  implying heat absorption, there is decrease of the fluid physical temperature. The effect of heat source parameter gives a similar behavior with both  $Fe_3O_4$  and  $TiO_2$  as solid mechanisms.

## 6. CONCLUSIONS

The RK4 scheme along with shooting technique was employed on the modified nonlinear ODEs to investigate the impacts of both the radiant heating and the thermal generation/absorption on the estimated solution of squeezed unstable nanofluid flow within two equidistant plates. The water like regular fluid and  $Fe_3O_4$  and  $TiO_2$  as the solid nano particles were considered and analyzed. The nondimensional velocity and temperature outlines have been studied. Moreover, it is quite ostensible that the moment nano particles are being augmented into the fluid, the heat transfer is enhanced, due to their great thermal conductivity feature. Thus, the desired and fascinating results were achieved numerically and graphically. The influences of all the prominent parameters concerned have been reviewed and exhibited thereof. The impacts of all the pertinent parameters present have been reported and presented both in tabular and graphically.

## Competing Interests

The authors declare that they have no competing interests.

## REFERENCES

- [1] H. Saleh, E. Alali, and A. Ebaid, "Medical applications for the flow of carbon-nanotubes suspended nanofluids in the presence of convective condition using Laplace transform", *Journal of the Association of Arab Universities for Basic and Applied Sciences*, 24(1), 2017, 206–212.
- [2] F. C. Lai, and F.A. Kulacki, "Non-Darcy mixed convection along a vertical wall in a saturated porous medium", *Journal of Heat Transfer*, 113, 1991, 252–255.
- [3] Ali J. Chamkha, "On laminar hydromagnetic mixed convection flow in a vertical channel with symmetric and asymmetric wall heating conditions", *International Journal of Heat and Mass Transfer*, 45, 2002, 2509–2525.
- [4] J.C. Umarathai, A.J. Chamkha and A. Mateen, "Unsteady two-fluid flow and heat transfer in a horizontal channel", *Heat Mass Transfer*, 42, 2005, 81.
- [5] Salma Parvin, Rehena Nasrin, M.A. Alim, N.F. Hossain, Ali J. Chamkha, "Thermal conductivity variation on natural convection flow of water–alumina nanofluid in an annulus" *International Journal of Heat and Mass Transfer*, Volume 55, Issues 19–20, 2012, pp.5268-5274.
- [6] M. Ghalambaz, SAM. Mehryan, and E. Izadpanahi, "MHD natural convection of Cu-Al<sub>2</sub>O<sub>3</sub> water hybrid nanofluids in a cavity equally divided into two parts by a vertical flexible partition membrane", *Journal of Thermal Analysis and Calorimetry*, 138 (2), 2019, pp. 1723-1743.
- [7] J. Raza, F. Mebarek-Oudina, and A.J. Chamkha, "Magneto-hydrodynamic flow of molybdenum disulfide nanofluid in a channel with shape effects", *Multidiscipline Modeling in Materials and Structures*, Vol. 15 No. 4, 2019, pp. 737-757.
- [8] B. Kumar, G.S. Seth, R. Nandkeolyar, and A.J. Chamkha, "Outlining the impact of induced magnetic field and thermal radiation on magneto-convection flow of dissipative fluid", *International Journal of Thermal Sciences*, Volume 146, 106101, ISSN 2019, 1290-0729.
- [9] Ali J. Chamkha, A.S. Dogonchi, and D.D. Ganji, "Magneto-hydrodynamic flow and heat transfer of a hybrid nanofluid in a rotating system among two surfaces in the presence of thermal radiation and Joule heating" *AIP Advances*, Volume 9, 025103; 2019, doi: 10.1063/1.5086247.
- [10] D. Tohraie, R. Mashayekhi, H. Arasteh, S. Sheykhi, M. Niknejadi, and A.J. Chamkha, "Two-phase investigation of water-Al<sub>2</sub>O<sub>3</sub> nanofluid in a micro concentric annulus under non-uniform heat flux boundary conditions" *International Journal of Numerical Methods for Heat & Fluid Flow*, Vol. 30 No. 4, 2020, pp. 1795-1814.
- [11] M. Molana, A.S. Dogonchi, T. Armaghani, Ali J. Chamkha, D.D. Ganji, and Iskander Tlili, "Investigation of Hydrothermal Behavior of Fe<sub>3</sub>O<sub>4</sub>-H<sub>2</sub>O Nanofluid Natural Convection in a Novel Shape of Porous Cavity Subjected to Magnetic Field Dependent (MFD) Viscosity" *Journal of Energy Storage*, Volume 30, 2020.

[12] A. S. Dogonchi, M. K. Nayak, N. Karimi, Ali J. Chamkha, and D. D. Ganji, "Numerical simulation of hydrothermal features of Cu–H<sub>2</sub>O nanofluid natural convection within a porous annulus considering diverse configurations of heater", *J. Therm. Anal. Calorim.*, 2020, DOI: 10.1007/s10973-020-09419-y.

[13] Nirmalendu Biswas, U. K. Sarkar, Ali J. Chamkha, and Nirmal Kumar Manna, "Magneto-hydrodynamic thermal convection of Cu-Al<sub>2</sub>O<sub>3</sub>/water hybrid nanofluid saturated with porous media subjected to half-sinusoidal nonuniform heating", *Journal of Thermal Analysis and Calorimetry*, 143: 2021, 1727–1753.

[14] M. Sheikholeslami, D.D. Ganji, and H.R. Ashorynejad, "Investigation of squeezing unsteady nanofluid flow using ADM", *Powder Technol.* 239, 2013, 259–265.

[15] E.A. Hamza, "The magneto hydrodynamic effects on a fluid film squeezed between two rotating surfaces", *J. Phys. D: Appl. Phys.* 24, 1991, 547–554.

[16] R. Kandasamy, I. Muhaimin, A.B. Khamis, and R. Roslan, "Unsteady Hiemenz flow of Cu-nanofluid over a porous wedge in the presence of thermal stratification due to solar energy radiation: lie group transformation", *Int. J. Therm. Sci.*, 65, 2013, 196–205.

[17] T. Hayat, A. Qayyum, F.E. Alasaadi, M. Awais, and D. Abdullah, "Thermal radiation effects in squeezing flow of a Jeffery fluid", *European Physical Journal Plus*, 128 (8), 2013, DOI: 10.1140/epjp/13085-1.

[18] A. Alsaedi, M. Awais, and T. Hayat, "Effects of heat generation/absorption on stagnation point flow of nanofluid over a surface with convective boundary conditions", *Commun. Nonlinear Sci. Numer. Simulat.*, 17, 2012, 4210–4223.

[19] S.A. Hussaini, Sher Muhammad, Gohar Ali, Syed Inayat Ali, Mohammed Ishaq, Zahir Shah, Hameed Khan, and Muhammad Naeem, "A bioconvection Model for squeezing flow between parallel plate containing Gyrotactic Microorganisms with impact of thermal Radiation and Heat Generation Observation" *Journal of Advances in mathematics and computer science*, 27 (4), 2018, 1-22.

[20] A.H. Srinivasa, and A.T. Eswara, "Effect of internal heat generation or absorption on MHD free convection from an isothermal truncated cone", *Alexandria Eng. J.*, 55, 2016, 1367–1373.

[21] M.S. Abdel-wahed, E.M.A. Elbashbeshy, and T.G. Emam, "Flow and heat transfer over a moving surface with non-linear velocity and variable thickness in a nanofluid in the presence of Brownian motion", *Appl. Math. Comput.*, 254, 2015, 49–62.

[22] A.G. Madaki, R. Roslan, M.S. Rusiman, and C.S.K. Raju, "Analytical and numerical solutions of squeezing unsteady cu and TiO<sub>2</sub> –nanofluid flow in the presence of thermal radiation and heat generation/absorption", *Alexandria Engineering Journal*, 57, 2018, pp.1033-1040.

[23] G. Domairry, and A. Aziz, "Approximate analysis of MHD squeeze flow between two parallel disks with suction or injection by homotopy perturbation method", *Math. Probl. Eng.*, 2009, 603916.

[24] S. Rosseland, *Astrophysik und atom-theoretische grundlagen*, "Springer Verlag", Berlin, 1931, pp. 41–44.

[25] N.S. Akbar, S. Nadeem, R.U.I. Haq, and Z.H. Khan, "Radiation effects on MHD stagnation point flow of nanofluid towards a stretching surface with convective boundary condition", *Chin. J. Aeronaut.* 26 (6), 2013, 1389–1397.

[26] M. Kothandapani, and J. Prakash, "Effects of thermal radiation parameter and magnetic field on the peristaltic motion of Williamson nanofluids in a tapered asymmetric channel", *Int.J. Heat Mass Transf.* 81, 2015, 234–245.

[27] M. Mustafa, T. Hayat, and S. Obaidat, "On heat and mass transfer in the unsteady squeezing flow between parallel plates", *Meccanica* 47, 2012, 1581–1589.